Publications

Available Online

J. Sci. Res. 5 (2), 301-314 (2013)

JOURNAL OF SCIENTIFIC RESEARCH

www.banglajol.info/index.php/JSR

Photocatalytic Degradation of Different Dyes Using TiO_2 with High Surface Area: A Kinetic Study

M. Z. B. Mukhlish*, F. Najnin, M. M. Rahman, M. J. Uddin

Department of Chemical Engineering and Polymer Science, Shahjalal University of Science and Technology, Sylhet 3114, Bangladesh

Received 18 August 2012, accepted in final revised form 24 January 2013

Abstract

Nanocrystalline TiO_2 was synthesized by using one step sol-gel method and characterized by SEM, XRD and EDS. UV-Vis spectroscopic technique has been used for studying the photocatalytic degradation kinetics of methylene blue (MB) and congo red (CR). A comparative study with commercial TiO_2 (P25) was also done to find out the effectiveness of this synthesized TiO_2. The synthesized TiO_2 exhibited a high photocatalytic activity for the degradation of MB and CR but the commercial TiO_2 was more efficient.

Keywords: Nanocrystalline TiO_2; Methylene Blue; Congo Red; Photocatalytic degradation kinetics.

doi: http://dx.doi.org/10.3329/jsr.v5i1.11641 J. Sci. Res. **5** (2), 301-314 (2013)

1. Introduction

A variety of physical, chemical, and biological methods, such as coagulation, adsorption, membrane process, and oxidation-ozonation are presently available for treatment of dye wastewater [1-3]. The conventional processes are insufficient to purify the wastewaters. They transfered the compounds from aqueous to another phase, thus causing secondary pollution problem. Photocatalytic oxidation is cost effective and capable of degrading any complex organic chemicals when compared to other purification techniques. TiO_2 is an important photocatalyst due to its strong oxidizing power, non-toxicity and long term photostability [4]. The TiO_2 catalyst can transform organic pollutants into biodegradable compounds of low molecular weight. A considerable technical and academic interest in the photocatalytic properties of nanosize TiO_2 powder has led to many detailed studies of the photodegradation of dyes and the related mechanisms and kinetics study [5-10]. TiO_2 particles smaller than tens of nanometers shows special optical properties, high catalytic

*Corresponding author: zobayer_ceps@yahoo.com

activity and unusual mechanical properties compared with bulk material counterpart [11]. Many methods have been developed to control the size of nanoparticles such as Langmuir-Blodgett films [12], vesicles [13], and reverse micro emulsions method [14]. The chemical and physical properties exhibited by these materials depend, among others, on the composition and the degree of homogeneity. Therefore, different synthesis strategies have been developed such as co-precipitation, flame hydrolysis, impregnation, chemical vapor deposition etc. [15, 16]. The sol-gel method has demonstrated a high potential for controlling the bulk and surface properties of the oxides [17, 18]**.** Nonhydrolytic sol-gel routes have been also reported in the literature [18, 19].

In this work, we focus on the preparation of TiO_2 by sol-gel process. The aims of our study are: (a) to synthesize TiO_2 nanoparticles from titanium iso-butoxide (TiB) by one step sol-gel method, (b) to characterize the morphology and structure of the prepared TiO_2 with several physical methods (SEM, XRD, EDS) and (c) to investigate the photocatalytic degradation kinetics using MB and CR. The photo catalytic performance of P25 is also studied and compared with that of synthesized TiO_2. The experimental kinetic data are fitted to various kinetic models and model parameters are evaluated.

2. Experimental

2.1. *Materials*

Titanium isobutoxide (Alfa Aesar, USA), 2-propanol (Alfa Aesar, USA), methylene blue (MERCK, Germany), and congo red (MERCK, Germany) were used as received. Water used in our experiments was triple distilled before use.

2.2. *Synthesis*

The synthesis reactor consists of a three necked round flask equipped with a vertical condenser fitted to the middle neck. A separatory funnel was connected to one of the two side necks. 24.13 mL of deionized water was added to 102.34 mL of 2-propanol under vigorous stirring to the remaining neck of the reactor. Following the addition of water this neck was closed using a rubber stopper. 50 mL of titanium isobutoxide (TiB) was added drop wise to the solution over a 4 h period using the separatory funnel fitted to the flask. This mixture was stirred continuously over a period of 24 h at room temperature under inert condition. At this stage, a stable colloidal suspension of approximately 175 mL was formed. The excess water and alcohol were removed at room temperature and 10 kpa pressure using a rotavapor (Buchi R2015) over a seven days period. Approximately 20 g of TiO_2 was obtained using this procedure.

2.3. *Photocatalytic experiment*

0.5 g of TiO_2 was taken into different ceramic crucibles and calcined in a muffle furnace (JSMF-30T, Korea) for 3 h at 450°, 550° and 650°C respectively. Then the TiO_2 samples were cooled to room temperature and placed into 50 mL beaker. Thereafter 5 ppm of MB or CR solutions were prepared in 100 mL volumetric flask. UV-Vis spectra were recorded using UV-spectrophotometer (UV-1650, SHIMADZU, Japan) in the wavelength range of 200-800 nm. After that, 50 mL of dye (MB or CR) solution was poured into each beaker that contains TiO_2 powders. The solution was placed under solar-like light. Samples were withdrawn at appropriate time intervals and concentration of dye in the solution was determined by UV-spectrophotometer. The same experimental procedure was followed for P25 to compare with the synthesized one.

2.4. *The degradation kinetic models*

Four kinetics models were used to analyse the kinetic data of MB and CR photocatalytic degradation on TiO_2 [20-23] :

i. The zero-order model describes the degradation process and can be generally expressed as,

$$c - c_0 = -kt \tag{1}$$

ii. The first-order model describes the systems where degradation rate depends on the amount of dye molecules in the solution and represented as,

$$\log(c/c_0) = -kt \tag{2}$$

iii. The parabolic diffusion model elucidates the diffusion controlled photodegradation and the equation can be written as follows,

$$\frac{1-(c/c_0)}{t} = -kt^{-1/2} + a \tag{3}$$

iv. The modified Freundlich model represented by Eq. (4) explains experimental data in terms of ion exchange and diffusion-controlled process. A good fit into the Freundlich model indicates a heterogeneous surface binding.

$$\log(1-\frac{c}{c_0}) = \log k + b\log t \tag{4}$$

In these equations, C_0 and C are the concentration of dye molecule in the solution at time 0 and t, respectively, k the corresponding rate constant, and a and b constants whose chemical significance is not clearly resolved [20].

2.5. *Characterization techniques*

Scanning electron microscopy (SEM) was performed using HITACHI-4800**.** JEOL 2010, operated at 200 kV and equipped with an energy dispersive spectroscopic (EDS) microanalysis system (OXFORD). The images are obtained using a CCD Mega Vision (III) camera. The X-ray diffraction (XRD) patterns were obtained using a Brucker D-5000 diffractometer equipped with Cu-kα radiation of wavelength of 1.5418 Aº. The accelerating voltage and the applied current were 45 kV and 40 mA, respectively.

3. Results and Discussions

3.1. *Morphology and structure analysis*

SEM image of the TiO_2 particles synthesized by sol gel chemistry at low temperature is shown in Fig. 1. It shows the uniformity of the aggregates that are in the nanoscale range. The TiO_2 aggregates consist of individual nanoparticles, which are approximately in the 50-60 nm range. The nanostructured surface of the individual particles suggests that pollutant molecules impinging or adhering to the surface should interact preferentially with the photoactive TiO_2 phase.

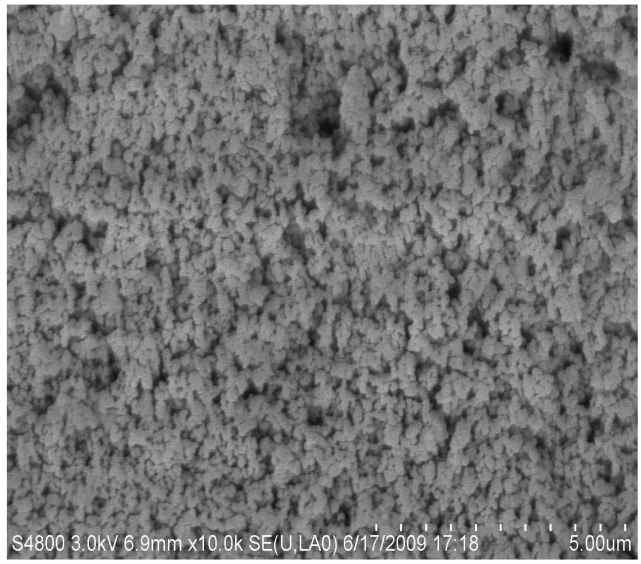

Fig. 1. SEM image of nanostructured TiO_2 aggregates.

EDS is an analytical technique used for the elemental analysis of a sample. The EDS spectra of the prepared TiO_2 sample are shown in Fig. 2, which clearly confirm the

presence of titanium and oxygen. The other peaks corresponding to '*' and 'C' are due to supporting materials used in EDS analysis. This implies that TiO_2 sample prepared at low temperature under vacuum condition is free from contamination.

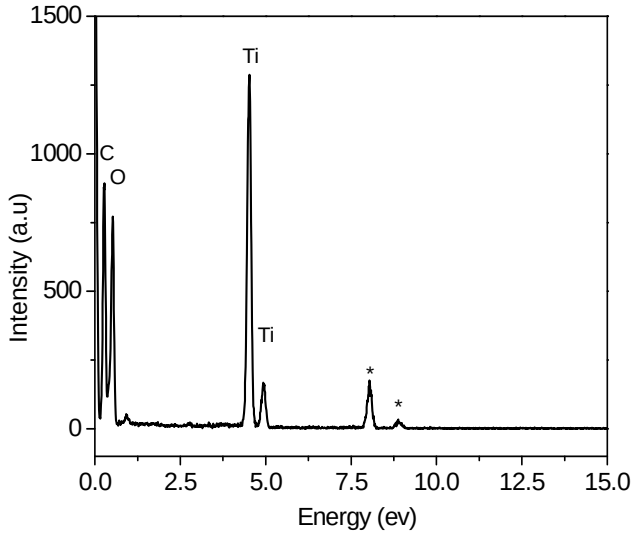

Fig. 2. EDS spectrum of synthesized TiO_2 sample. Ti and O indicate the presence of titanium and oxygen. (C and * represent carbon and copper that come from analysis grid).

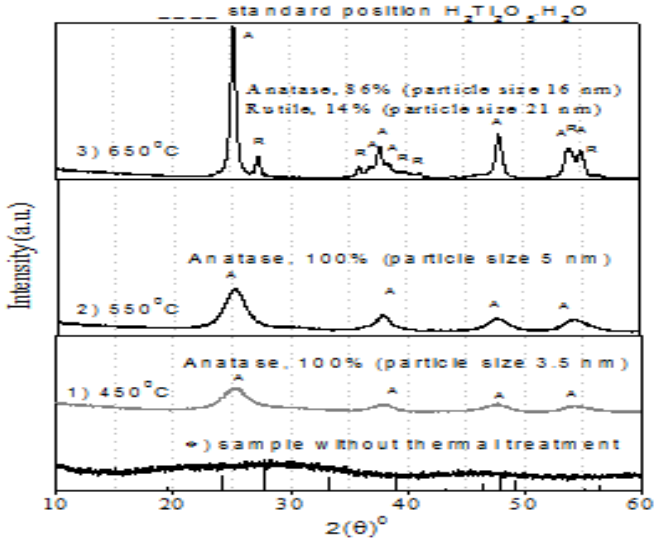

Fig. 3. XRD patterns of TiO_2 sample calcined at (1) 450°C, (2) 550°C, (3) 650°C, and (*) sample without thermal treatment. (A: anatase phase; R: rutile phase).

The XRD patterns of synthesized titania matrix calcined at different temperatures are reported in Fig. 3 (Curve 1-3). Curves 1 and 2 report three broad peaks and one intense peak at 38.01°, 47.5°, 54.20° and 25.1°, which are firmly indicative of TiO_2 of anatase phase [17]. Additionally curve (3) shows a few small peaks at 27.3°, 36.0° and 39.60°, and 41.2° which are closely related to rutile phase. No additional peaks belonging to other phases are observed. The remarkable width of the peaks associated with the TiO_2 phase suggests that the size of the particle is quite small (Fig. 3, curve 1 and 2). From full width at half maxima (FWHM) of the peaks at 25.1° and 38.01° and by using Scherrer's equation, $Lc = K\lambda/(\beta \cos \theta)$ [24] (where λ is the X-ray wavelength, β is the FWHM of the diffraction line, θ is the diffraction angle, and K is a constant, which has been assumed to be 0.9), the average particle diameter of about 4 nm can be calculated. This result is strongly consistent with the SEM result described above. In conclusion, by comparing the results coming from the different techniques, it comes out that the investigated samples contain nanosized anatase particles of size (~4 nm). Of course, curve 3 gives a certain amount (14%) of rutile phase due to calcining the sample at high temperature (650°C). The XRD pattern of sample without thermal treatment is shown as pattern (*, Fig. 3). It is revealed that the sample contains only hydrogen titanate which is confirmed by the standard sample analysis (the vertical lines).

3.2. *Photocatalytic activity*

The UV-Vis absorption spectra with increasing illumination time are shown in Figs. 4, 5 and 6. Fig. 4 shows the decrease of MB band on TiO_2 sample upon solar-like light

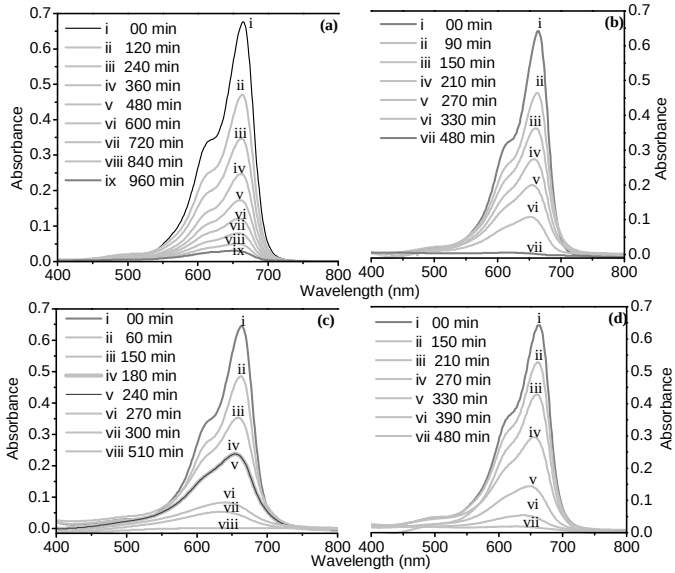

Fig. 4. UV-vis spectral changes of MB spectra under solar-like light exposure using (a) TiO_2 (without thermal treatment), TiO_2 calcined at (b) 450°C, (c) 550°C and 650°C.

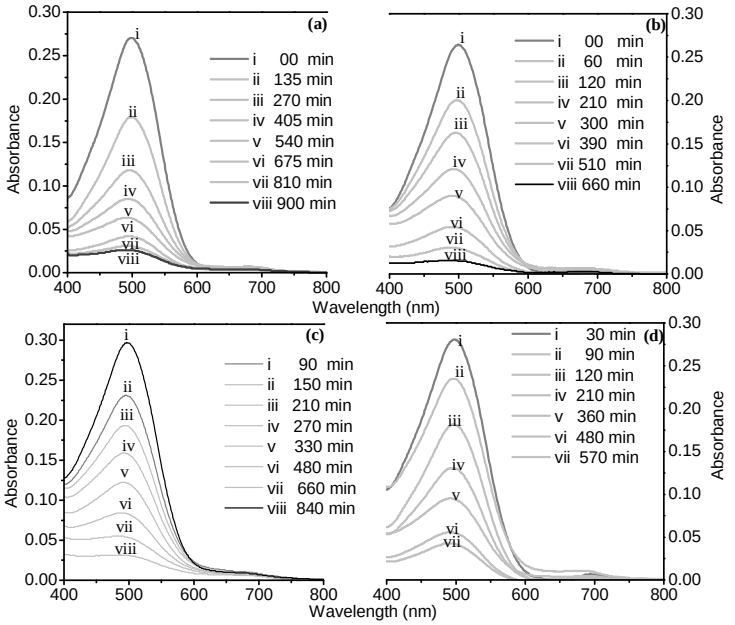

Fig. 5. UV-vis spectral changes of congo red spectra under solar-like light exposure using (a) TiO_2 (without thermal treatment), TiO_2 calcined at (b) 450°C, (c) 550°C and 650°C.

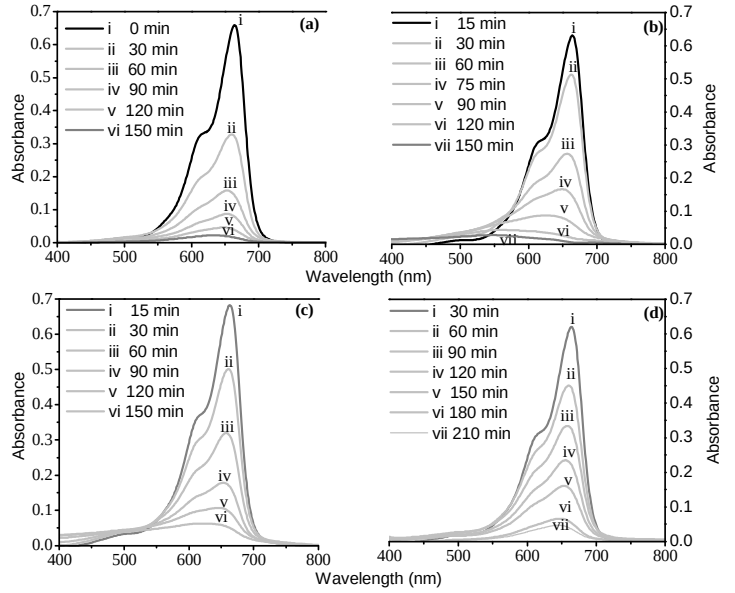

Fig. 6. UV-vis spectral changes of methylene blue spectra under solar-like light exposure using (a) P25 (without thermal treatment), P25 calcined at (b) 450°C, (c) 550°C and 650°C.

exposure while Fig. 5 shows the same using CR on TiO_2. Fig. 6 reports the photocatalytic activity of P25, the best TiO_2 photocatalyst on MB under solar-like light illumination. The maximum UV-Vis absorptions for MB and CR are at the wavelength of 664 nm and 498 nm respectively. The maximum absorption occurred almost at the same wavelength throughout the photo degradation period. The absorption band in the range of 500-750 nm was observed for MB (Figs. 4 and 6) while for CR it was in the range of 400-600 nm (Fig. 5). The absorbance of the spectra rapidly decreased with increasing irradiation time (Figs. 4-6) and the peak of spectra almost disappeared after few hours solar irradiation as TiO_2 promotes catalytic photo degradation of dyes. This is not unexpected since the photo catalytic activity of TiO_2 is well known [17]. The chromophores responsible for characteristic color of the dyes (MB and CR) were broken down and the dyes were degraded with time. The disappearance rate of the absorption band due to MB adsorbed on P25 is much faster than that observed in case of synthesized TiO_2. A small band around 600 nm wavelength for both case of TiO_2 (P25) and synthesized TiO_2 was observed because two aromatic rings in MB starts to degrade creating a mono substituted molecule. This indicates that the photodegradation not only destroys the conjugate system (including −N=N−) but also breaks down partially or totally the intermediate products [19-25]. Comparing the two dyes, it is observed that chemical structure of MB lends itself more to oxidation by hydroxyl radicals, than does CR. Moreover, it is possible that MB absorbs less UV light than CR. This would make more photons available to impinge on the catalyst and promote the formation of hydroxyl radicals. However it must be acknowledged that the degradation comparisons between the two dyes are made on a mass basis. On a molecular basis the analysis is much different. MB and CR have molecular weights of 320 and 697 respectively. The pohotoatalytic degradation kinetics of MB and CR on TiO_2 samples and reference P25 are shown in Figs. 7a-c. It can be inferred that degradation of dye (MB or CR) is slower with noncalcined TiO_2 compared to the calcined sample. About 91% degradation of MB (Fig. 7a) is observed within 420 and 780 min. in presence of calcined and noncalcained TiO_2 sample, respectively. About 90% degradation of CR (Fig. 7b) is achieved within 570 min. for TiO_2 calcined at 650°C, while the same percentage of degradation requires 660 and 780 min. for TiO_2 calcined at 450° and 550°C, respectively. Calcination at higher temperature causes dehydration of TiO_4H_8 ($TiO_4H_8 \rightarrow TiO_2 + H_2O$) producing more active sites and consequently, enhances adsorption and photodegradation. An important result obtained from Fig. 7c is that the noncalcined TiO_2 (P25) particles are comparatively more active in MB degradation than calcined particles. P25 calcined at the highest temperature (650°C) shows the lowest degradation performance among the calcined samples. This is not unexpected. Commercial TiO_2 contains both anatase and rutile phases. The photocatalytic activity of anatase is higher than rutile nanocrystalline TiO_2 [4]. As TiO_2 is calcined at high temperature some anatase particles are transformed into rutile phase causing lower performance in MB degradation.

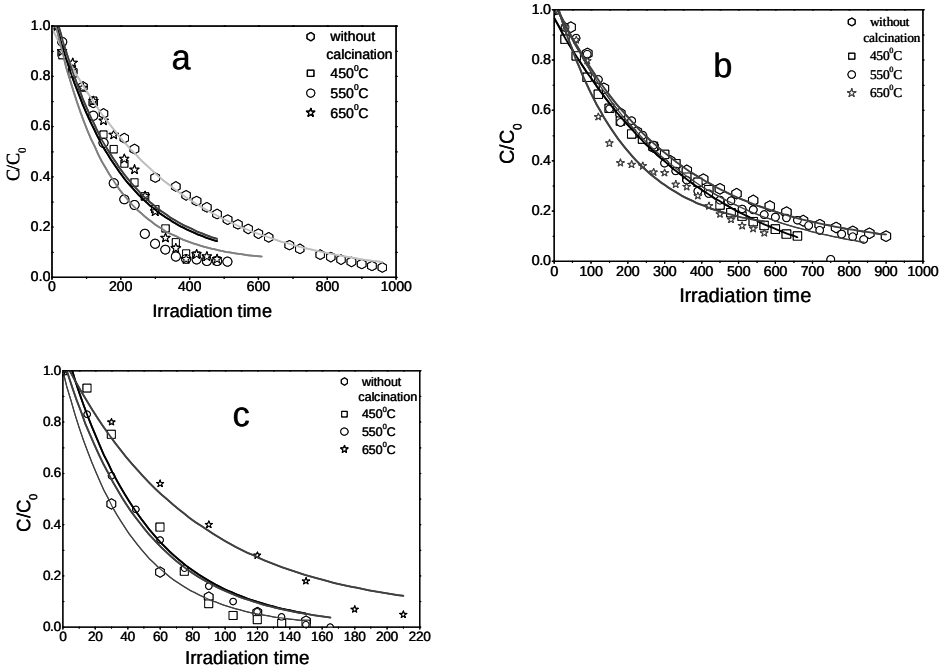

Fig. 7. Photocatalytic degradation kinetics of a) MB, and b) CR on TiO_2 sample, and c) MB on TiO_2 (P25) calcained at 450°C, 550°C and 650°C.

3.3 *Photocatalytic degradation kinetic models*

The experimental kinetic data were treated with four types of kinetic models (zoro-order, first-order, parabolic-diffusion, and modified Freundlich model, Figs. 8-10) to investigate the mechanism of successive adsorption and degradation process. The model parameter *k* as well as the correlation coefficient (R^2) are shown in Tables 1-3.

The kinetic data of the MB and CR adsorption simultaneous photodegradation on TiO_2 and P25 are well described by the Modified Freundlich and first order models. From Figs. 10 and 11, it can be observed that the adsorption kinetics of MB and CR on the as-synthesized titanate nanoparticles may be described more precisely by the Modified Freundlich model and the dyes are adsorbed to the titanate surface by monolayer adsorption [26] and the molecules follow successive photocatalytic degradation. The zero-order and parabolic-diffusion models were not suitable to explain the whole photocatalytic degradation process. The modified Freundlich model fits the kinetic data with linear correlation coefficient of R^2 = ~0.99 (Table 1) for MB and R^2 = ~0.99 (Table 2) for CR photocatalytic degradation using synthesized TiO_2. The modified Freundlich model, in fact, describes heterogeneous diffusion from the flat surface via molecular ion exchange. Moreover, the kinetic model prediction suggests similarities in the photocatalytic activity

of synthesized TiO_2 and P25. The modified Freundlich model fits the kinetic data with R^2 = ~0.97≈0.98 for MB degradation using P25.

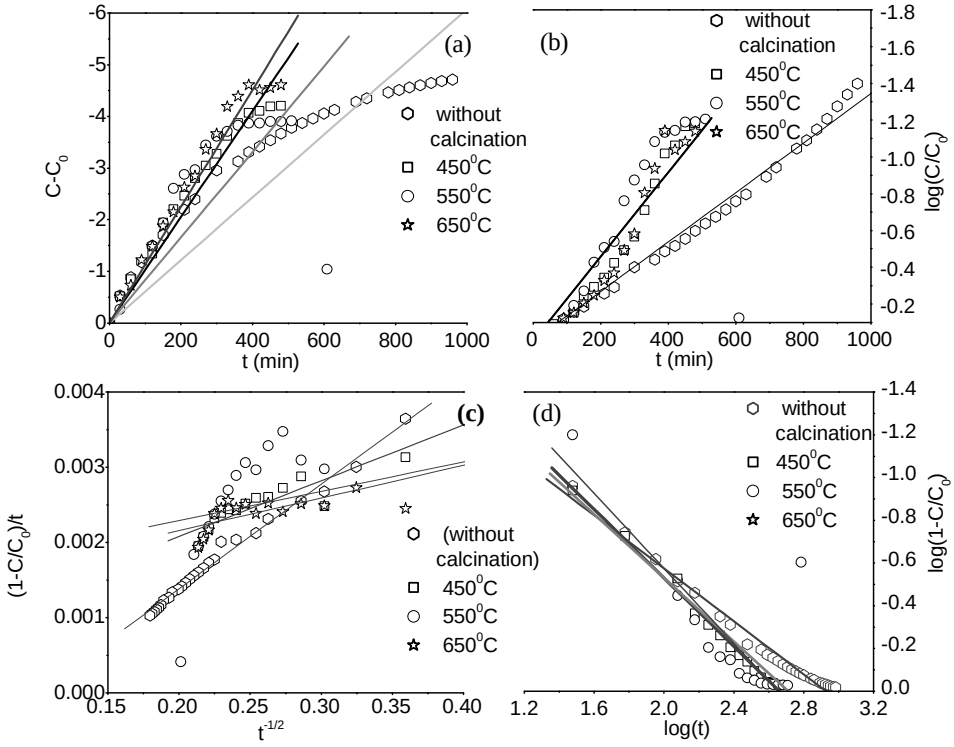

Fig. 8. Photocatalytic degradation Kinetics of (a) Zero-order, (b) First-order, (c) Parabolic diffusion (d) Modified-Freundlich model of MB on TiO_2 and TiO_2 calcined at 450°C, 550° and 650°C.

Table 1. Linear correlation coefficients (R^2) and rate constant (k) of the zero-order (mol $L^{-1}m^{-1}$), first-order (m^{-1}), parabolic diffusion (mg $kg^{-1}s^{-0.5}$) and modified Freundlich ($Lg^{-1}m^{-1}$) kinetic models for photo catalytic degradation of MB on TiO_2 (without thermal treatment) and TiO_2 calcined at 450°C, 550°C and 650 °C.

Kinetic Models	Without calcination		450°C		550°C		650°C	
	R^2	k	R^2	k	R^2	k	R^2	k
Zero order	0.903	0.0061	0.968	0.0102	0.374	0.0083	0.807	0.0113
First order	0.991	0.00134	0.960	0.0023	0.446	0.0022	0.942	0.0023
Parabollic diffusion	0.949	0.0108	0.846	0.0047	0.343	0.0073	0.661	0.0044
Modified Freundlich	0.993	0.0153	0.991	0.0073	0.987	0.0095	0.988	0.0047

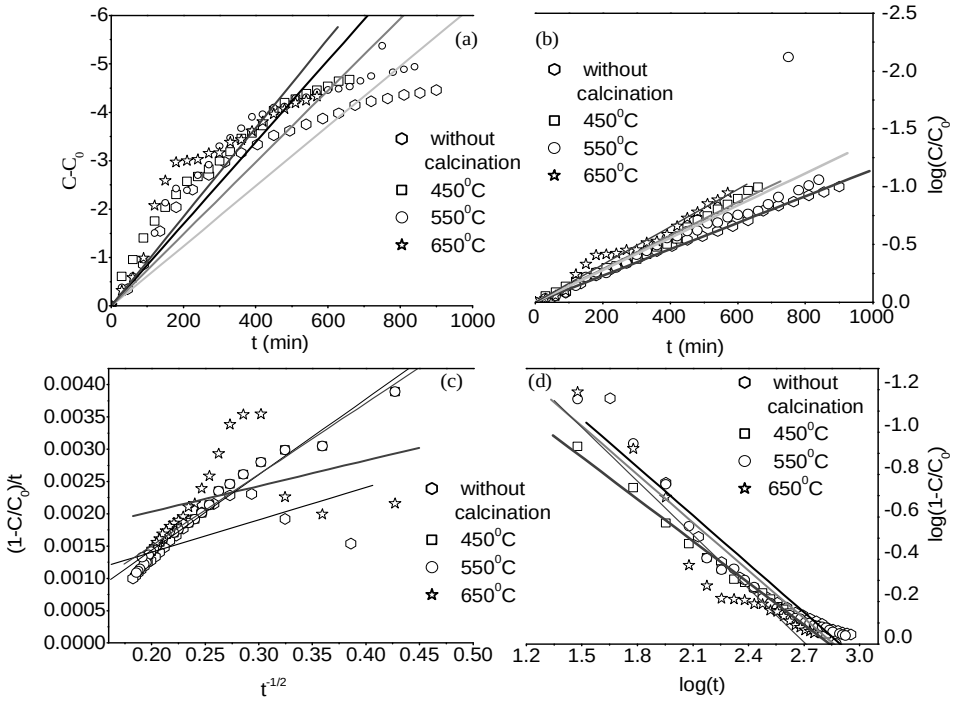

Fig. 9. Photocatalytic degradation kinetics of (a) Zero-order, (b) First-order, (c) Parabolic diffusion (d) Modified-Freundlich model of CR on TiO_2 (without thermal treatment) and TiO_2 calcined at 450°C, 550°C and 650°C.

Table 2. Linear correlation coefficients (R^2) and rate constant (k) of the zero-order (mol $L^{-1}m^{-1}$), first-order (m^{-1}), parabolic diffusion (mg $kg^{-1}s^{-0.5}$) and modified Freundlich ($Lg^{-1}m^{-1}$) kinetic models for photo catalytic degradation of CR on TiO_2 (without thermal treatment) and TiO_2 calcined at 450°C, 550° and 650°C.

Kinetics model	Without calcination		450ºC		550ºC		650ºC	
	R^2	k	R^2	k	R^2	k	R^2	k
Zero order	0.8784	0.0062	0.951	0.0085	0.8751	0.0074	0.756	0.0092
First order	0.996	0.00115	0.987	0.00144	0.755	0.0014	0.973	0.0016
Parabollic diffusion	0.631	0.005	0.942	0.011	0.800	0.011	0.364	0.00397
Modified Freundlich	0.995	0.00626	0.996	0.0135	0.988	0.0069	0.987	0.0052

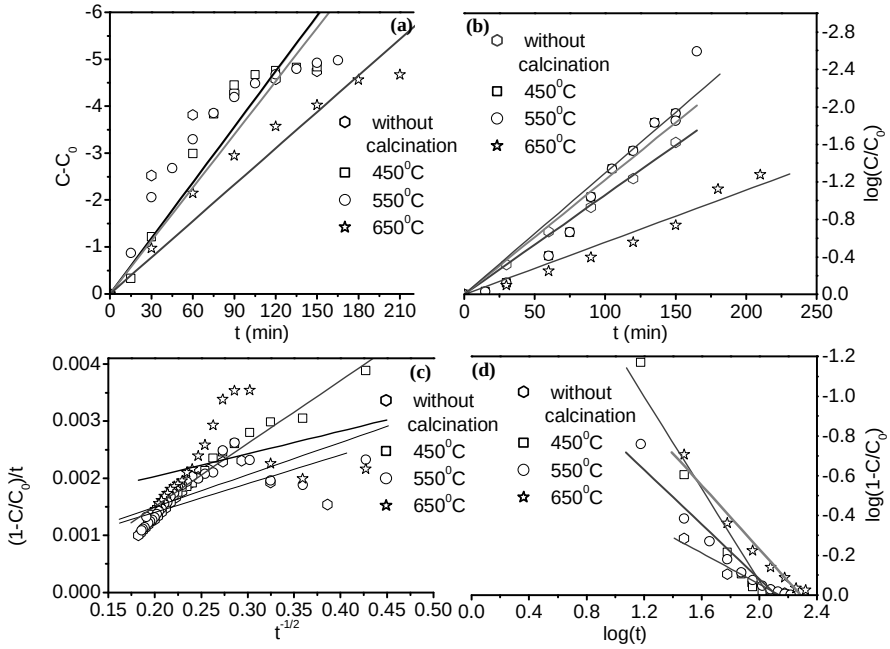

Fig. 10. Photocatalytic degradation kinetics of (a) Zero-order, (b) First-order, (c) Parabolic diffusion (d) Modified-Freundlich model of MB on TiO_2 (P25) and TiO_2 (P25) calcined at 450°C, 550° and 650°C.

Table 3. Linear correlation coefficients (R^2) and rate constant (k) of the zero-order (mol $L^{-1}m^{-1}$), first-order (m^{-1}), parabolic diffusion (mg $kg^{-1}s^{-0.5}$) and modified Freundlich ($Lg^{-1}m^{-1}$) kinetic models for photo catalytic degradation of MB on TiO_2 (P25) and TiO_2 (P25) calcined at 450°C, 550° and 650°C.

Kinetic Model	Without calcination		450°C		550°C		650°C	
	R^2	k	R^2	k	R^2	k	R^2	k
Zero order	0.800	0.0394	0.903	0.0395	0.879	0.0377	0.949	0.0258
First order	0.997	0.0106	0.966	0.0122	0.910	0.012	0.968	0.0055
Parabolic diffusion	0.631	0.005	0.942	0.0110	0.742	0.0057	0.364	0.0039
Modified Freundlich	0.970	0.1456	0.975	0.0407	0.968	0.034	0.984	0.0145

4. Conclusion

Photocatalytic degradation using TiO_2 is successfully applied for the textile dyes (MB and CR). The results confirm that the sol-gel method is a good way to prepare anatase TiO_2 nanoparticle. The prepared TiO_2 shows a high photocatalytic activity for the degradation of MB and CR. The decolorization and degradation efficiency depend upon the

calcinations of catalyst. In this study it is observed that the first order and Freundlich model fit the kinetic data well. Though commercial TiO_2 is more efficient, the synthesized TiO_2 can also effectively remove the dyes (MB and CR) from wastewater.

References

1. P. S. Kumar, S. Ramalingam, C. Senthamarai, M. Niranjanaa, P. Vijayalakshmi, and S. Sivanesan, Desalination **252**, 149 (2010). http://dx.doi.org/10.1016/j.desal.2009.10.010
2. M. S. I. Mozumder and M. A. Islam, J. Sci. Res. **2**, 567 (2010). http://dx.doi.org/10.3329/jsr.v2i3.4302
3. M. A. M. Arami, N. M. Mahmoodi, and A. Akbari, Desalination **267**, 1107 (2010).
4. R. J. Tayade, P. K. Surolia, R. G. Kulkarni, and R. V. Jarsa, Sci. Technol. Adv. Mater. **8**, 455 (2007). http://dx.doi.org/10.1016/j.stam.2007.05.006
5. C. H. Hung, P. C. Chiang, C. Yuan, and C. Y. Chou, J. Water Sci. Technol. **2**, 313 (2001).
6. C. Nasr, K. Vindgopal, S. Hotchandani, A. K. Chattopadhyay, and P. V. Kamat, Res. Chem. Inter. **23**, 219 (1997). http://dx.doi.org/10.1163/156856797X00439
7. K. Vinodgopal, I. Budja, and P. V. Kamat, Chem. Mater. **8**, 2180 (1996). http://dx.doi.org/10.1021/cm950425y
8. M. M. Alam, M. Z. Bin Mukhlish, S. Uddin, S. Das, K. Ferdous, M. M. R. Khan , and M. A. Islam, J. Sci. Res. 4, 665 (2012). http://dx.doi.org/10.3329/jsr.v4i3.8654
9. S. Somekawa, Y. Kusumoto, H. Yang, M. Abdulla-Al-Mamun, and B. Ahmmad, J. Sci. Res. 2, 17 (2010). http://dx.doi.org/10.3329/jsr.v2i1.2992
10. M. S. Anwer, S. Kumar, F. Ahmed, N. Arshi, C. G. Lee, and B. H. Koo, J. Nanosci. Tecnol. **12**, 1555 (2012). http://dx.doi.org/10.1166/jnn.2012.4634
11. R. W. Siegel, Ann. Rev. Mater. Sci. **21**, 559 (1991). http://dx.doi.org/10.1146/annurev.ms.21.080191.003015
12. H. Y. Kyunghee, J. H. Fendler, Langmuir **6**, 1519(1990). http://dx.doi.org/10.1021/la00099a015
13. H. C. Youn, S. Baral, and J. H. Fendler, J. Phys. Chem. **92**, 6320 (1988). http://dx.doi.org/10.1021/j100333a029
14. J. H. Fendler, Chem. Rev. **87**, 877(1987). http://dx.doi.org/10.1021/cr00081a002
15. M. Toba, F. Mizukami, S. Niwa, T. Sano, K. Maeda, A. Annila, and V. Komppa, J. Molec. Catal. **1**, 277 (1994). http://dx.doi.org/10.1016/0304-5102(94)00040-9
16. X. Gao, and E. Wachs, Catal. Today **51**, 233(1999). http://dx.doi.org/10.1016/S0920-5861(99)00048-6
17. M. J. Uddin, F. Cesano, F. Bonino, S. Bordiga, G. Spoto, D. Scarano, and A. Zecchina, J. Photochem. Photobiol. A-Chem. **189**, 286 (2007). http://dx.doi.org/10.1016/j.jphotochem.2007.02.015
18. M. J. Uddin, F. Cesano, S. Bertarione, F. Bonino, S. Bordiga, D. Scarano, and A. Zecchina, J. Photochem. Photobiol. A-Chem. **196**, 165 (2008). http://dx.doi.org/10.1016/j.jphotochem.2007.07.037
19. F. Cesano, S. Bertarione, M. J. Uddin, G. Agostini, D. Scarano, and A. Zecchina, J. Phys. Chem. C **114**, 169 (2009).
20. D. L. Sparks, *Harcourt. Jovanovich Publishers: San Diego*, (1989), Kinetics of Soil Chemical Process.
21. Z. H. Li, Langmuir **15**, 6438 (1999). http://dx.doi.org/10.1021/la981535x
22. E. Demirbas, M. Kobya, E. Senturk, and T. Ozkan, Water SA. **30**, 533 (2004). http://dx.doi.org/10.4314/wsa.v30i4.5106
23. T. Kodama, Y. Harada, M. Ueda, K. Shimizu, K. Shuto, and S. Komarneni, Langmuir **17**, 488 (2001). http://dx.doi.org/10.1021/la001774w
24. L. S. Birks and H. Friedman, J. Appl. Phys. **17** 687 (1946). http://dx.doi.org/10.1063/1.1707771

25. S. Al-Oaradawi and S. R. Salman, J. Photochem. Photobiol. A **148**, 161 (2002). http://dx.doi.org/10.1016/S1010-6030(02)00086-2
26. Y. W. L. Lim, T. Yuxin, Y. H. Cheng, and Z. Chen, Nanoscale **2**, 2751 (2010). http://dx.doi.org/10.1039/c0nr00440e